

SIMULATION ANALYSIS DESIGN EXPERIMENTAL OF NATURAL GAS – DIESEL OXIDATION IN FLEX FUEL ENGINE

Nnadikwe Johnson¹ Chuku Dorathy E. Jerry² Ewelike Asterius Dozie³ Samuel H. Kwelle⁴

¹Department of Petroleum and Gas Engineering Imo State University, Owerri, Nigeria

²Department of Petroleum and Gas Engineering Federal University Otuoke Bayelse State

³H.O.D department of Agriculture and Environmental Engineering, Imo State University, Owerri, Nigeria

⁴First Independent Power Limited, Rivers State, Nigerian

ABSTRACT

Research into alternative fuel oxidation methods has been driven by recent stringent pollution legislation and the desire to reduce global CO₂. The use of dual-fuel technology improves thermal efficiency and reduces pollution by using two fuels instead of one. Because of its low price and relatively low environmental impact, natural gas is a viable short-term solution. In a compression ignition engine, natural gas may improve performance while decreasing carbon dioxide emissions. Inefficient oxidation of natural gas-diesel fuel and increased emissions of unburned hydrocarbons and carbon monoxide occur under low engine loads. This report presents the findings of experimental and modeling studies of natural gas-diesel dual-fuel operations in three engine designs. Diesel infusion and air-path techniques on reduced-zone oxidation performance were investigated using a multi-cylinder engine, as well as two single-cylinder engines with and without visual access. Low-load, clean oxidation is made possible by injection pressure and diluting the input charge. Better diesel injection might lead to more consistent combustion and better cylinder oxidation. In order to lower NO_x emissions and improve thermal efficiency of brakes, significant quantities of exhaust gas recirculation are needed.

Keywords: natural gas, diesel, dual-fuel, engine oxidation, simulation

INTRODUCTION

For almost a century, the diesel engine, also known as an ignition engine, has been an essential part of the global energy infrastructure. Because of growing environmental concerns and government restrictions to promote clean energy alternatives, the CI engine's role in the next sustainable energy economy is under doubt.

As part of the Paris Agreement, emissions of greenhouse gases need to be reduced by 40% by 2030 (UNFCC, 2015). Using renewable eco-friendly fuels like hydrogen and ammonia in a CI engine's dual-fuel mode may cut CO₂ emissions, sometimes by more than the target amount. Only 5% of the world's hydrogen is produced through water electrolysis, whereas 95% is produced from fossil fuels like natural gas and coal (IRENA, 2019).

With lower carbon dioxide (CO₂) emissions than other petroleum-derived fuels, compressed natural gas (CNG) is a viable short-term choice for a CI engine's primary fuel source. As a result of its low cost and adaptability, natural gas is a popular option. Because of its high autoignition limit, natural gas cannot be compressed and oxidized (Sahoo et al., 2009) unless it is mixed with diesel.

Natural gas is injected into the intake manifold or intake ports to provide a uniform charge within the cylinders during this oxidation mode. Primitive diesel fuel oxidation sets off a natural gas-air mixture that is otherwise homogenous (Wei and Geng, 2016). The thermal efficiency of dual-fuel natural gas-diesel engines

exceeds that of spark-ignition CNG engines (Kojima et al., 2016). Since methane, the primary component of compressed natural gas (CNG), has one of the lowest carbon contents among hydrocarbons, it is possible that CNG dual-fuel engines will minimize CO₂ emissions in comparison to diesel engines. As the engine is able to run on more natural gas, it is able to reduce CO₂ emissions even while under heavier loads (Lounici et al., 2014).

The amount of diesel used and the operating conditions will determine how much of an impact natural gas has on NO_x output in a dual-fuel engine. When operating at lower loads, dual-flex engines emit fewer nitrogen oxides (NO_x) than conventional engines. Possible causes for the decrease include a lower in-cylinder temperature because natural gas has a higher specific heat capacity than air, and a longer ignition delay, both of which decrease oxidation efficiency (Wei and Geng, 2016). Larger amounts of heat released in the premixed oxidation zone, followed by a quicker pressure rise rate and higher in-cylinder temperatures, are often to blame for NO_x degradation at higher engine loads (Selim, 2001).

Since it contains neither aromatics or sulfur, natural gas is more conducive to flames involving premixed oxidation and less diffusion, which results in less soot (Maricq et al., 2002). Several researchers (Liu et al., 2013) confirm this. Unburned methane is cited as a major source of CO and HC emission penalties in the published literature (Shenghua et al., 2003; Cheenkachorn et al., 2013; Liu et al., 2013).

When under little load, the dual-fuel engine struggles. Large CNG-to-diesel energy sharing ratios result in significant carbon monoxide and unburned hydrocarbon emissions at low equivalence ratios. Diesel fuel's poor and slow oxidation of lean natural gas-air mixtures is to blame for the increase in emissions (Tsujimura et al., 2012). (Lounici et al., 2014). Brake thermal efficiency (BTE) in dual-fuel engines is reduced by 50% when compared to diesel, as shown by Papagiannakis et al. (2010). At 95% of maximum load, Abdelaal and Hegab (2012) were only able to improve dual-fuel engine BTE by 3%. Increasing the proportion of diesel to compressed natural gas (CNG) might solve this issue, but it would reduce CNG's benefits and raise CO₂ emissions (Kojima et al., 2016).

In recent years, several studies have been conducted to better understand how to enhance low-load zone oxidation. Pilot diesel's effect on unburned hydrocarbons was investigated by Liu et al. (2013). According to the research, increased diesel consumption decreased HC concentrations. Even still, 90% of HC emissions were from methane that was never burnt. Diesels with an injection pressure between 46 and 72 MPa had better oxidation performance, as measured by a shorter ignition delay, a shorter oxidation time, and a higher BTE, according to a study by Yang et al. Although BTE production increased, high-pressure CO and THC emissions went up. It has been observed that high injection pressure led to spray impingement on the piston and cylinder wall. By timing diesel injection earlier and increasing intake gas temperature, Srinivasan et al. (2006) improved the oxidation efficiency of the dual-fuel engine. According to Kusaka et al. (1998), NO generation is minimal under light-load conditions. Preheating the intake air using EGR decreases nitrogen oxides and trichloroethene, and increases thermal efficiency.

In this piece, I'll be breaking down how a dual-fuel engine that uses natural gas and diesel performs in a variety of settings. The efficiency of the dual-fuel engine was measured using a variety of injection (pattern, timing) and airpath (EGR, boosting) procedures. The study area is the low-load, low-oxidation region. The current study offers experimental analysis with three different engine configurations and computational fluid dynamics (CFD) simulations.

EXPERIMENTAL APPARATUS

Extensive experimental findings across three power plant layouts are presented in this paper (Table 1). The oxidation process and the operation of single- and multi-cylinder engines were studied using a number of different engine layouts.

Both engines in Figure 1A and 1B have cylindrical combustion chambers and a visible crankshaft. No. 0 Solvent M was used in place of diesel since the ocular engine needed to be started from cold. Figure 1C depicts a multi-cylinder engine used to examine how different air-path approaches affect oxidation and emissions from a dual-fuel engine. Equipment comparisons for the three engine variations are shown in Figure 1.

Table 1: Details about each engine configuration

Test facility	Set-up #1	Set-up #2	Set-up #3
Engine type	4-Stroke single-cylinder diesel engine	4-Stroke single-cylinder diesel engine	4-Stroke 4-cylinder diesel engine
Bore x stroke (mm)	92 x 96	92 x 96	96 x 103
Displacement (cm ³)	638	638	2,981
Compression ratio	15:1	15:1	15:1
Combustion chamber	Dish (cavity φ : 56 mm)	Optical	Toroidal
Main fuel	CNG (port injection)	CNG (port injection)	CNG (port injection)
Pilot fuel	Diesel, CN: 56 (direct injection)	No. 0 Solvent M, CN: 89 (direct injection)	Diesel, CN: 56 (direct injection)
Injection system	Common rail @50 MPa	Common rail @50 MPa	Common rail @50 MPa
Nozzle type (inj. angle)	φ : 0.085 mm x 12 holes (θ : 130°)	φ : 0.085 mm x 12 holes (θ : 130°)	φ : 0.09 mm x 10 holes (θ : 155°)
Coolant temperature	80 ± 2	95 ± 2	80 ± 2

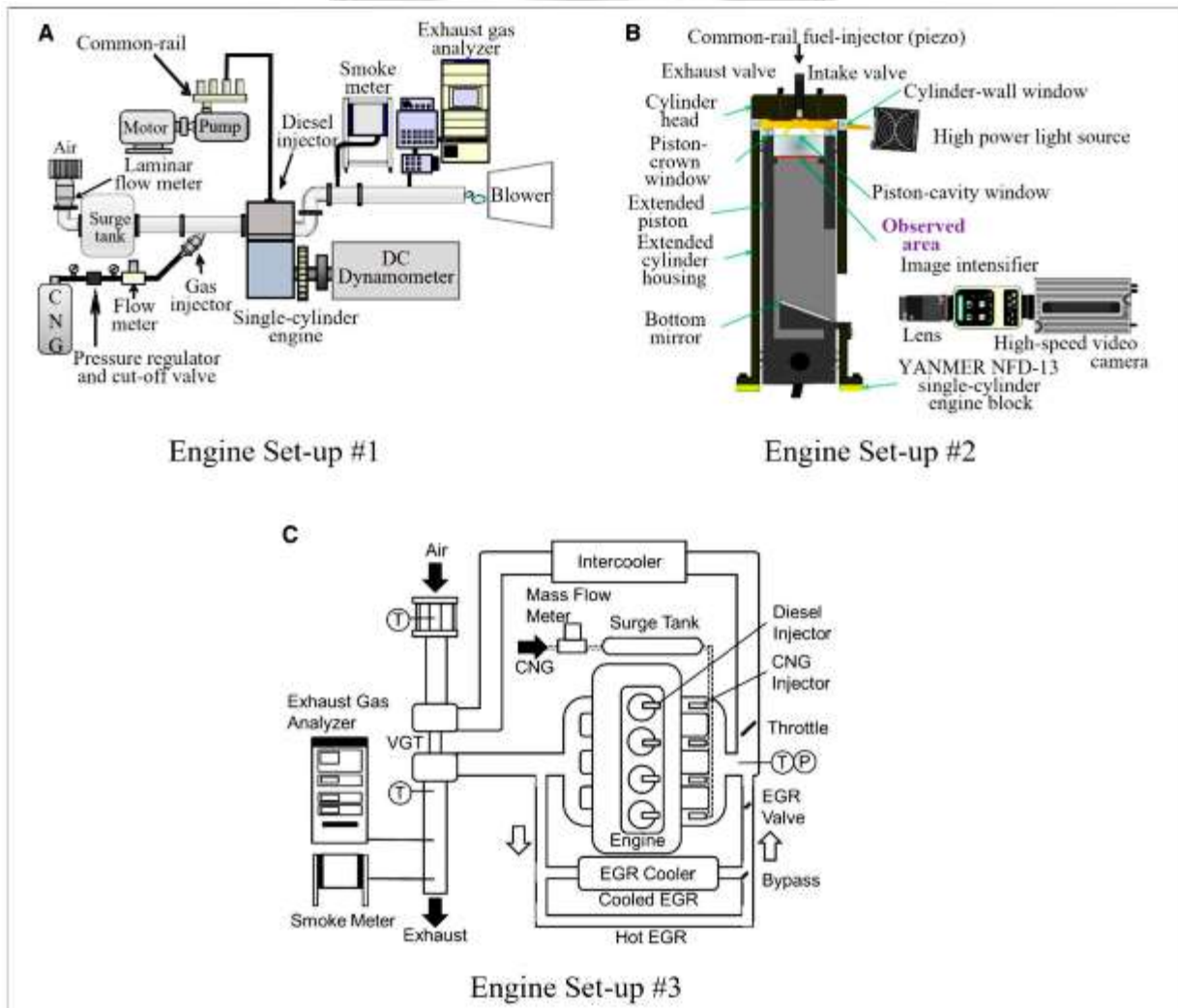


Figure 1: Facilities for conducting experiments: (A) set up a three-cylinder engine, (B) build up a single-cylinder engine with optical access, and (C) set up a three-cylinder engine with a common rail fuel injection system

The primary characteristics of natural gas and liquid fuels, as well as the three engine operating scenarios, are shown in and 3, respectively.

A Japan 13A natural gas injector was installed at the intake port of engine configurations 1 and 2 with a 638 cm³ expander. After opening the input valve, pressurized gas at 0.8 MPa was injected into the cylinder.

Table 2: The working conditions of the engines.

Test facility	Set-up #1	Set-up #2	Set-up #3
Engine speed (rpm)	1,200	1,200	1,200
BMEP/(IMEP) (MPa)	(0.05-1.1)	0.62/0.60	0.3
CNG air excess ratio	2.67	3	3.85
Diesel injection pattern	Single	Early single/split (double)	Single
Diesel injection timing (°CA ATDC)	-3, -13, -33, -53, -63	-60/-40+TDC	-22.5 to -2.5 (steps of 2.5)
Diesel amount (mm ³ /st)	2, 4, 10	10/5+5	5.7
Boost pressure (kPa)	100	100	100/120
EGR rate (%)	-	-	0, 10, 20, 30, 50

Table 3: Properties of fuel.

Fuel type	CNG (13A)	Diesel JIS (No. 2)	No. 0 Solvent M
Density (g/cm ³)	0.878	≈0.832	0.761
LHV ^a (MJ/kg)	52.47	43.12	43.8
CN ^b	-	56	89.4
Sulfur mass (ppm)	-	<50	<1
CNG composition	CH ₄ : 89.6%, C ₂ H ₆ : 5.62%, C ₃ H ₈ : 3.43%, C ₄ H ₁₀ : 1.35%		

^aLower heating value. ^bCetane number.

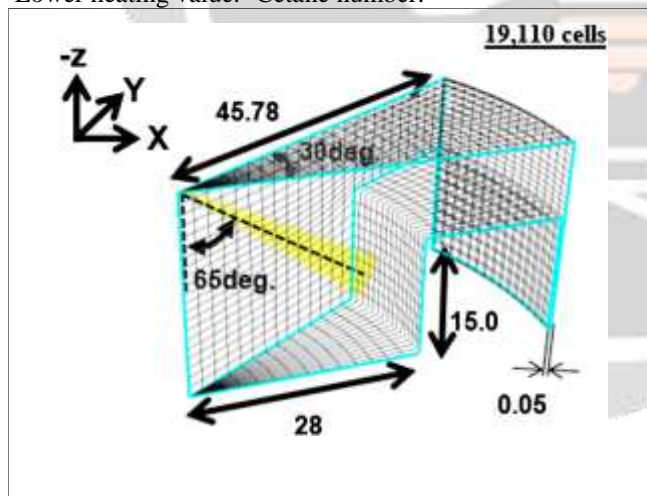


Figure 2: Grid for computational use (sector mesh at 30 degrees).

The cylinder's head is outfitted with a piezo diesel injector that has 12 holes and a 0.085 mm-diameter nozzle. All testing was conducted with diesel injection pressure set at 50 MPa on the in-house common-rail system. We measured the levels of exhaust gases using a HORIBA, MEXA-7000DEGR, and AVL 415S. See Engine Setup #2 in High Definition with This High-Speed Camera and Image Intensifier from FASTCAM APX RS with UVi-NAC Image Technology in Fig. 1B. CNG was supplied to the multi-cylinder engine through a surge tank connected to the intake manifold. If you look at Figure 1C, you can see how the timing of gas injection was adjusted to maintain a constant gas supply.

Exhaust smoke measurements from all three power plant layouts will not be provided in this research. All smoke levels were lower than 0.10 FSN [Filter Smoke Number specified by ISO 10054 (ISO 10054, 1998)], since the present study focuses on decreased operation with a limited diesel input amount.

COMPUTING FLUID DYNAMICS MODELING

Computing simulation research improved our understanding of oxidation in the cylinder. Figure 2 shows a cylinder embedded in a computational grid that was simulated using the FORTÉ program (Liang et al., 2010).

The alienation, sublimation, and instability sub-models in both KIVA-3V (Amsden, 1997) and FORTÉ are similar. To foretell how far a spray will go through a surface, researchers turned to the Kelvin-Helmholtz Rayleigh-Taylor (KH-RT) model (Reitz and Beale, 1999). The KH-RT model is sensitive to the relative velocities of the gas drops and the size of the mesh. For simulations that were not constrained by mesh size or time step, the gas jet model (Abani and Reitz, 2007) was used (Wang et al., 2010). To foretell oxidation processes, a turbulence interaction model was proposed by Kong and Reitz (2002). Incorrect mixing of fuel and oxidizer or oxidation products is assumed to lead to turbulent eddies, which in turn dictate some of the oxidation chemistry in this model. The relationship between the chemical time scale and the unstable scalar mixing time scale t_{mix} is analyzed. It is important to investigate the impact of mixing turbulence on species synthesis since computational cells are too small to represent actual turbulence and chemistry scales. The turbulence model requires a mixing time coefficient, C_{tki} , in order to be customized (ANSYS, Inc., 2019).

To further understand the effects of the C_{tki} on the model's ability to replicate experimental oxidation data, a parametric study was conducted as part of the dual-fuel study. The results of a simulation model with an early fuel injection at 60°CA after TDC are shown in Figure 3. (ATDC). Hot ignition at TDC is affected by C_{tki} level, however the low temperature response zone at 20°CA ATDC is unaffected. The results of this study, both theoretical and experimental, are most closely in line with a C_{tki} value of 1.

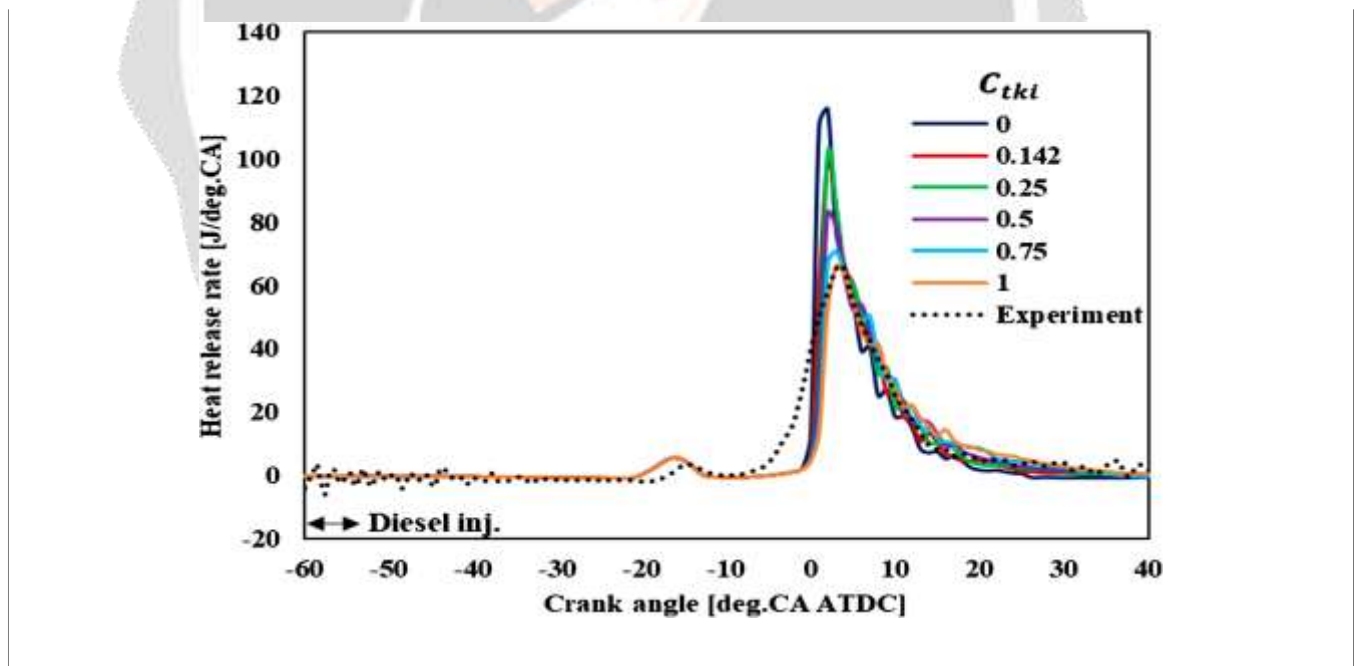


Figure 3: The influence of the C_{tki} parameter on the model's heat release prediction capability was studied metrically.

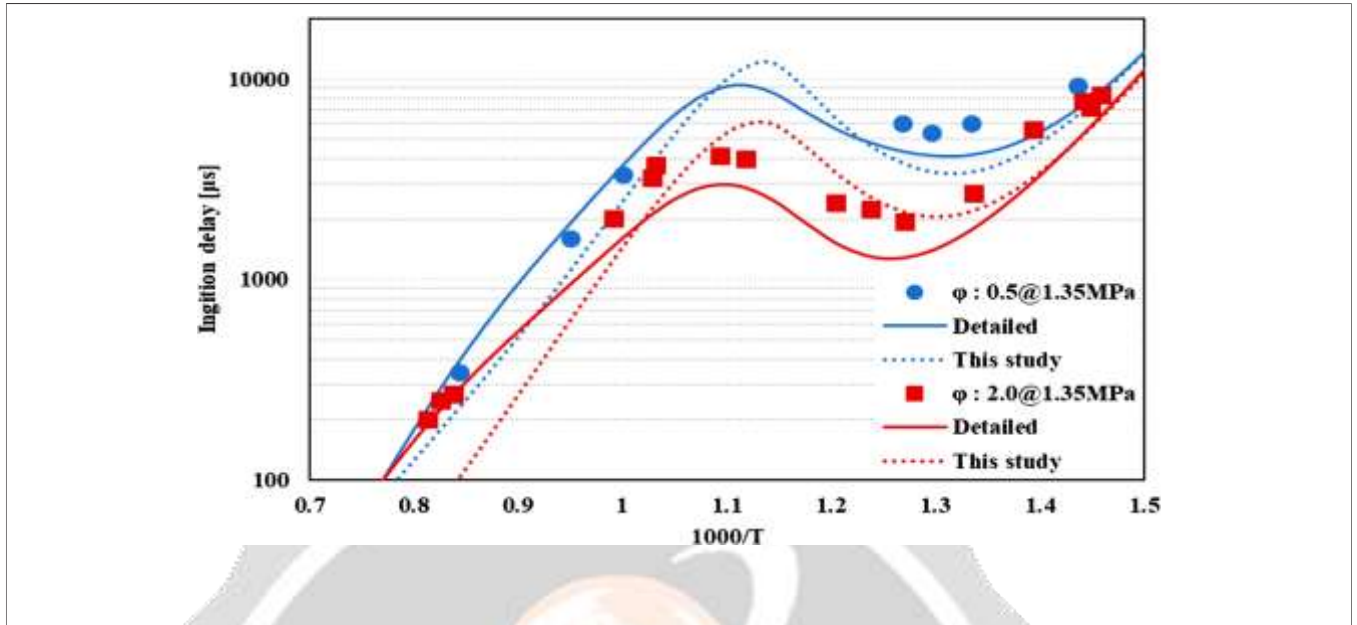


Figure 4: Correlation of the ignition timing of an n-heptane/air combination in a shock-tube environment computed using this study's simplified model and the full model (Mehl and Curran, 2009) with experimental findings (Ciezki and Adomeit, 1993)

Natural gas was modeled using the processes related with methane, which make up roughly 90% of its volume, while the diesel physical characteristics were modeled using a based on prior research (Patel et al., 2004; Mehl and Curran, 2009; Tsurushima, 2009). Species like methane, methyl radical, acetylene, and NOx inspired the authors to create a new, more efficient model for the synthesis of n-heptane/methane. There are 47 species in the updated model, and 87 reactions (Tsujiura et al., 2012).

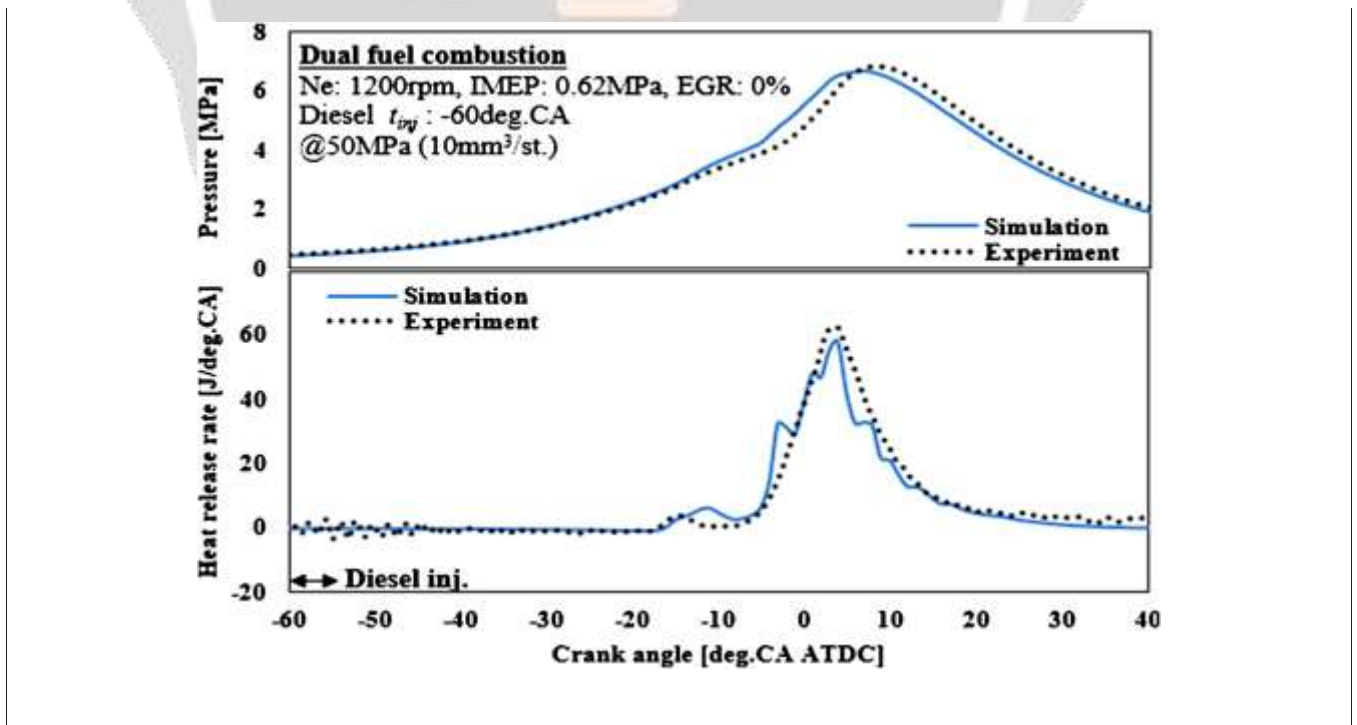


Figure 5: Experimental findings for early diesel infusion were compared to simulations of cylinder pressure and heat release.

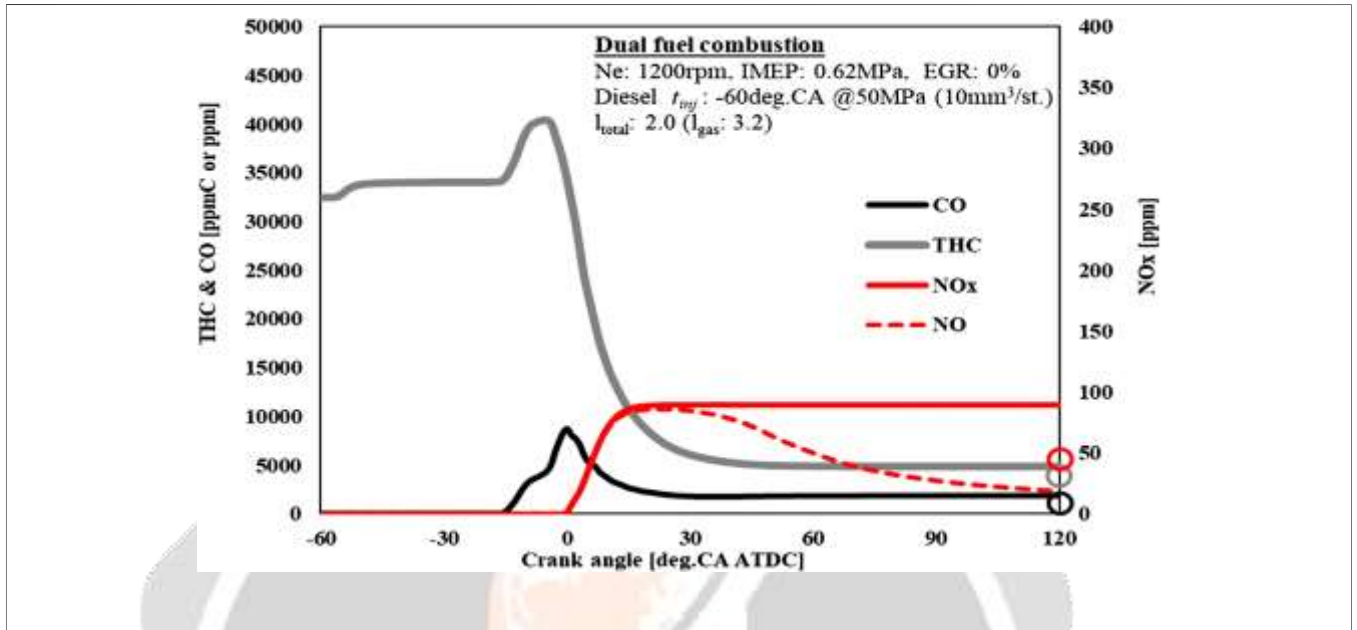


Figure 6: Comparison of early diesel intravenous experimental data (circles) with predicted emissions (CO, THC, NOx, and NO). When comparing the simple model of Ciezki and Adomeit to the full model, the results were found to be somewhat different (1993). Figure 4 shows that both models include 1,391 species and 5,935 characteristics, however the simpler model underestimates ignition delay at high temperatures.

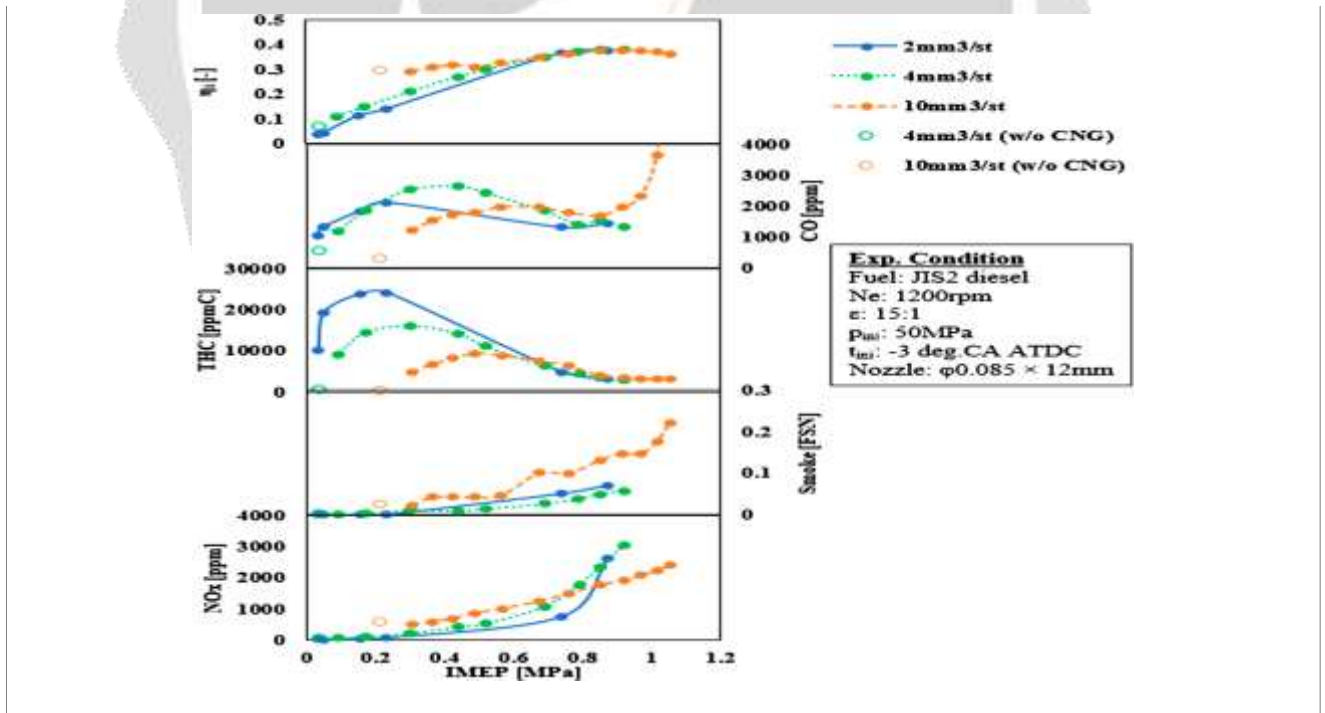


Figure 7: Characteristics of performance of dual-fuel engines at varying IMEPs and fuel-to-air ratios. The experimental findings at low temperatures agree with both the simple and the complete models. Experiment data from engine configuration #1 was compared to the simplified kinetic model utilized in the powerplant simulation scenario. Model validation for a 60°CA ATDC diesel injection is shown in Figure 5. The maximal

heat release ratio measured in the cylinder agrees very well with modeling results. Initial heat release, slope, and maximum level at low temperatures are all modeled. As can be seen in Figure 6, for all species except NO_x, computed emission patterns agree with experimental findings.

RESULTS AND DISCUSSION

All the experimental data presented here was gathered across three different engine configurations, providing a rich sampling of data from a variety of engine geometry configurations and direct observation of in-cylinder oxidation events. Additionally, computational fluid dynamics (CFD) simulations were utilized to learn more about oxidation and emission production.

Standard Operating Procedure

The dual fuel engine was compared to the standard single cylinder engine configuration 1. Natural gas flow rate was adjusted to meet engine power, and pilot diesel infusions of 2, 4, and 10 mm³/st at 3°CA ATDC were tried.

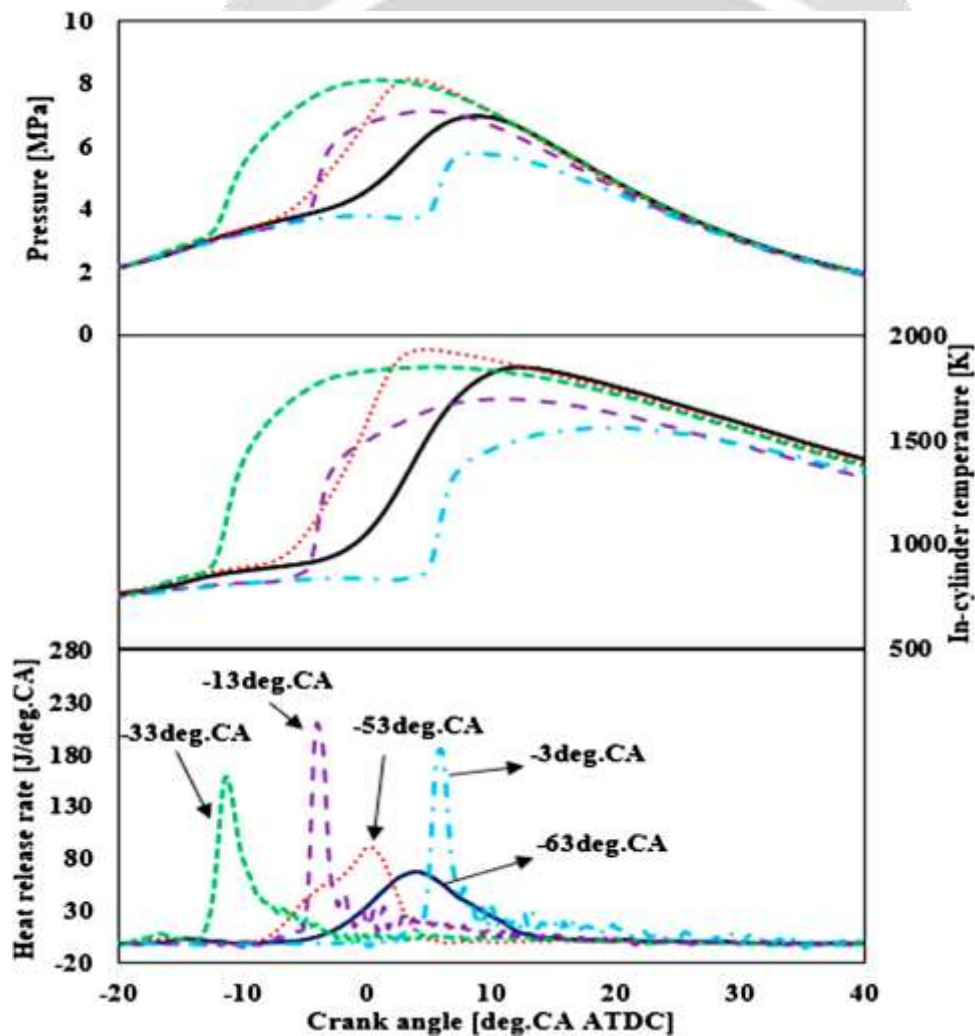


Figure 8: Changes in engine load, temperature, and release rate of heat in response to varying diesel injection times.

The thermal performance and emissions of the dual-fuel engine are shown for a range of pilot injection volumes and standard pressures in Figure 7. Better performance may be expected across the board when IMEP is increased. There is little effect of fuel amount in high IMEP situations. For better thermal efficiency, increase the amount of pilot injection when IMEP is low. Diesel fuel's ignitability is compromised by lean natural gas premixture conditions in the cylinder under light engine loads. In these conditions, the engine's oxidation efficiency increases as seen by a decrease in THCs when the diesel/natural gas energy sharing ratio is increased.

Diesel injection plans

Injection frequency

In the prior part, a constant diesel injection start was employed. For powerplant setting #1, the injection start angle was cranked up from 3°CA ATDC to 63°CA ATDC. In Figure 8, we see the average under-cylinder pressure and rate of heat release for diesel injection frequencies of 3, 13, 33, 53, and 63°CA ATDC, in situations of dual fuel oxidation.

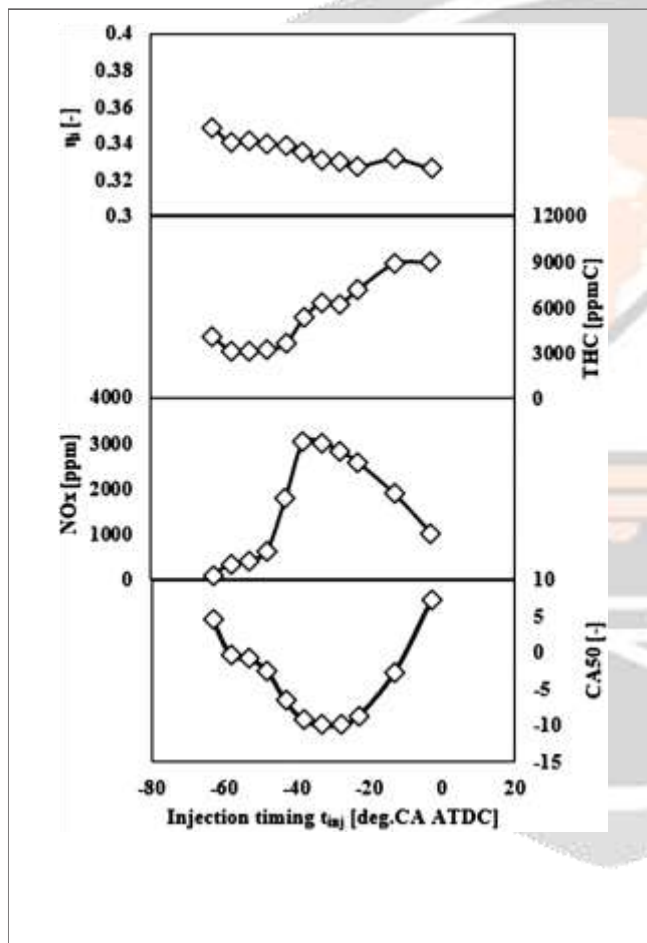


Figure 9: Dual-fuel engine thermal performance, total hydrocarbon emissions, nitrogen oxides, and cetane number at half-load as a function of diesel injection time (experimental conditions as shown in Figure 8)

Oxidation increased when diesel injection time moved beyond 3°CA ATDC (Figure 8). The heat release for the 13°CA example starts a few degrees CA before TDC and continues to rise sharply until it reaches the highest level of all cases. The lower rate of heat release at 33°CA was indicative of faster oxidation prior to TDC. With an initial injection temperature of 53 and 63°CA, oxidation was slowed and heat production was reduced. This shift in NOx emissions is seen in Figure 9. When diesel injection time is increased from 3 to 33°CA, NOx emissions increase. Reduced NOx emissions occur when the injection occurs as soon as possible. The CA50

graphic explains the NO_x behavior by showing the 50% oxidation region on the piston. Due to the quick release of heat, the 13°CA example has the earliest CA50 value. In-cylinder oxidation temperature and NO_x generation are both decreased at CA50 levels closer to TDC.

The thermal efficiency of the engine may be improved by injecting fuel early on. The ability to ignite the low natural gas combination is reduced because the diesel injection delay time is shortened by injecting diesel fuel later in the process. There may be less total hydrocarbons (THCs) in the exhaust if diesel is introduced early in the combustion process.

Half-Injection

As was discussed before, the performance and emissions of a diesel engine are affected by the injection time. Low oxidation efficiency from unburned fuel led to the production of high amounts of THCs during operation of a dual fuel engine under poor load conditions. In order to enhance diesel's ability to ignite natural gas under lean conditions, a split diesel injection method is presented in this section.

Oxidation was measured in-cylinder using Engine Setup #2 for this study. Diesel's capacity to ignite a low natural gas-air mixture is hindered by the fact that this kind of engine can only be evaluated under cold-start conditions. No. 0 Solvent M, which has a higher cetane number than diesel fuel, was used in this study.

In Figure 10, we see a comparison between (A) a single injection of 10 mm³ at 60°CA ATDC and (B) a split injection strategy in which 5 mm³ is injected at both 40°CA ATDC and TDC, and the resulting release rate heat and oxidation events.

Oxidation starts along the cylinder wall and squish area and spreads to the center of the cylinder in the first injection condition. The oxidation process in (A) started in the squish area, where a high concentration was found at the TDC, and progressed down the central axis of the oxidation chamber (Figure 11). While NO_x emissions may be as low as 45 ppm in the premixed oxidation condition, the flames still cover a significant portion of the cylinder chamber.

In the case of split injection, diesel is infused without any oxidation occurring beforehand. Bright diffusion flames erupt along the cylinder wall after the second injection, driving the heat release diagram sharply upward. For scenario (B), split injection, oxidation began in the primary chamber area, as shown in Figure 11. Case temperatures are increased because the second late injection produces fuel-rich zones in the oxidation chamber. After using split injection, the amount of NO_x produced by the engine is 758 ppm, which is roughly 15 times more than the amount produced by early injection.

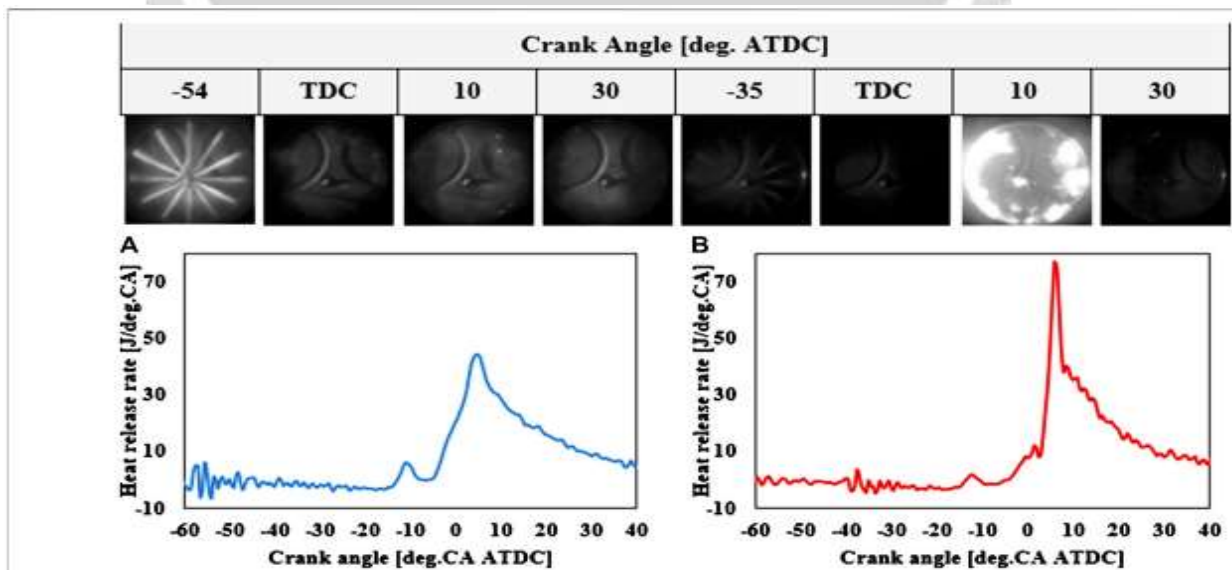


Figure 10: Heat release rate and in cylinder pictures for (A) initial fuel injection (IMEP 0.62 MPa, t_{inj} 60°ATDC, Q_d 10 mm³/cycle), and (B) divided injection (IMEP 0.60 MPa, t_{inj} 40°ATDC and TDC, Q_d 5 and 5 mm³/cycle).

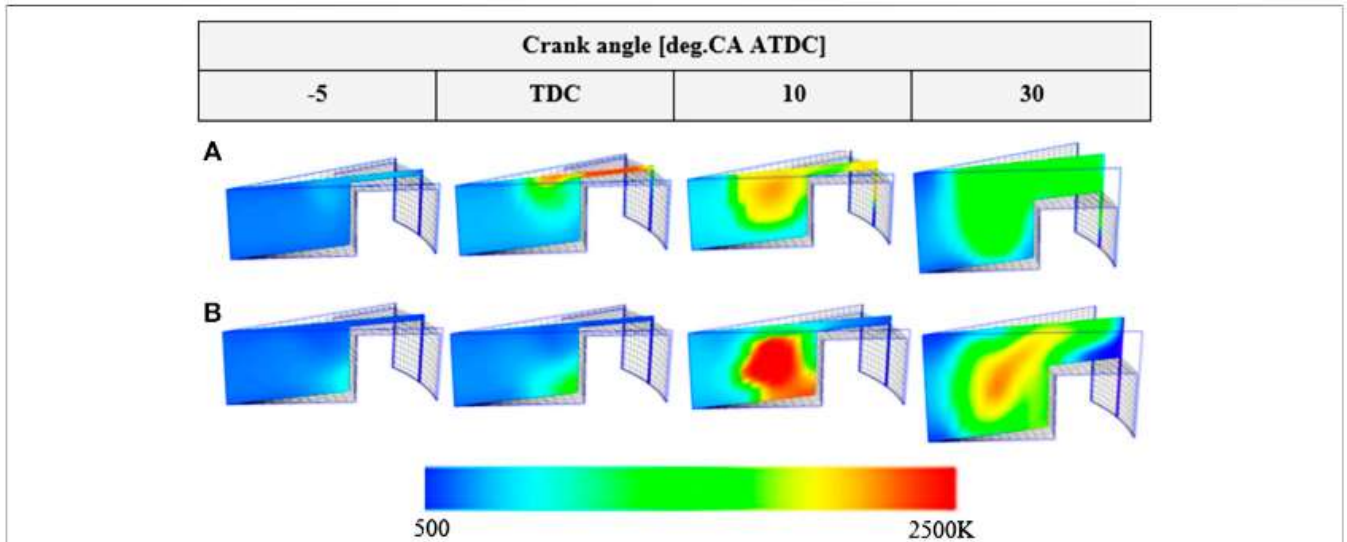


Figure 11: Plotting of in cylinder temperatures for (A) initial fuel infusion (IMEP 0.62 MPa, t_{inj} 60° ATDC, Q_d 10 mm³ /cycle), and (B) divided injection (IMEP 0.60 MPa, t_{inj} 40° ATDC and TDC, Q_d 5 and 5 mm³ /cycle).

See Figure 12 for a look at how the temperature profiles of different species relate to those of the two cases. In both cases, the amount of C₇H₁₆ decreases when heat is released at lower temperatures. More than two-thirds of the injection reactions in case (A) C₇H₁₆ and in case (B) initial occur before the zone of excessive heat release. The CH₄ profiles are steady until the point of maximum heat release. Case (A) homogeneous diesel/CNG combination covers a greater oxidation zone, resulting in more efficient CH₄ oxidation. When looking at hydrocarbon emissions and CH₄ profiles, it becomes clear that in both (A) and (B), 89% of UHC is a source of CH₄ (B). The release of low-temperature heat from C₇H₁₆ is the starting point for CO generation in both cases (LTHR). Since the following diesel infusion produces fuel-rich regions inside the cylinder, case (B) has greater CO.

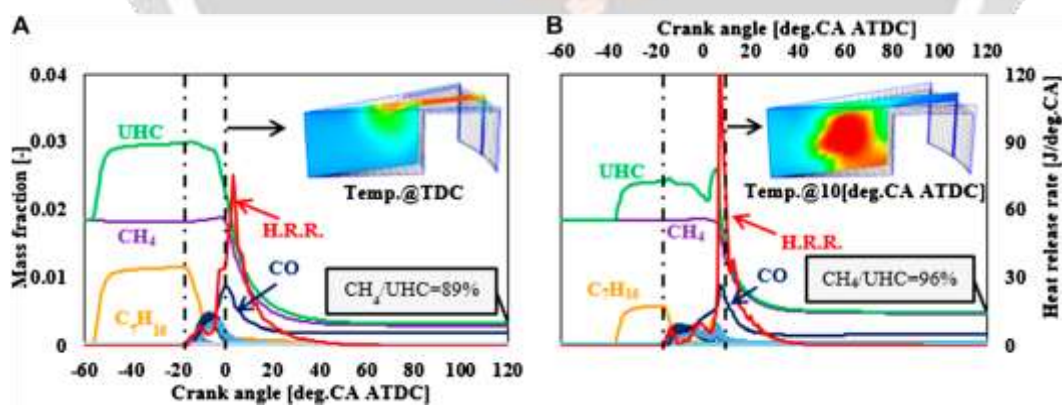


Figure 12: The major species and rate of heat release profiles are shown in (A) for the initial fuel injection scenario (IMEP = 0.62MPa, t_{inj} 60deg.ATDC, Q_d 10mm³/cycle), and (B) for the divided injection condition (IMEP = 0.60MPa, t_{inj} 40deg.ATDC & TDC, Q_d = 5 & 5 mm³/cycle).

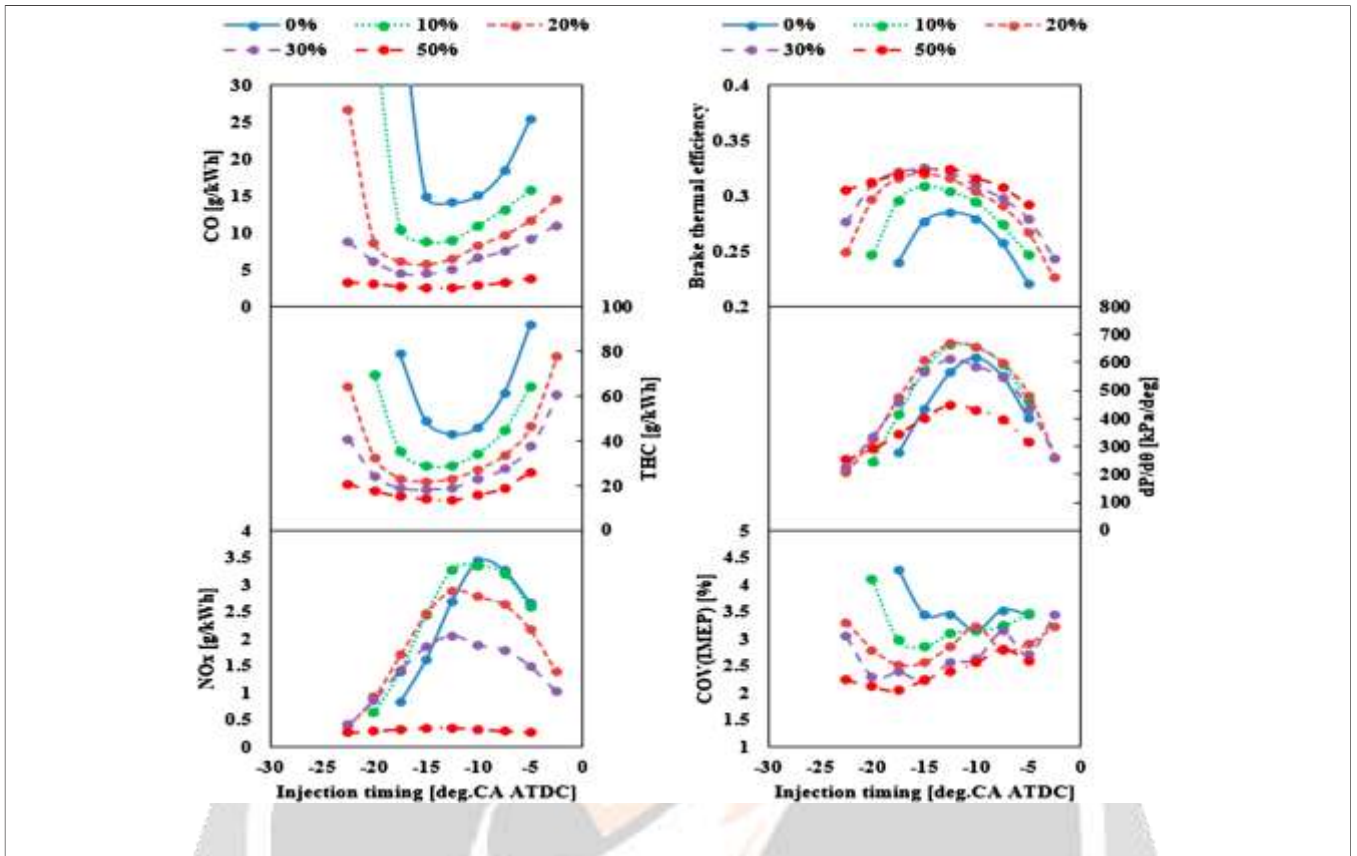


Figure 13: Differences in emissions and combustion efficiency at various diesel injection times and EGR ratios.

Air Route Planning

Different air-path techniques are examined in this part to see how they affect the efficiency and pollution levels of a natural gas-diesel a twin engine. Both exhaust gas recirculation (EGR) and inlet boosting (IB) were tested at 1,200 rpm. The third configuration of the multi-cylinder powertrain was chosen for the research because it is compatible with the turbocharger and high-pressure Hot-EGR system. The low-load engine zone with a 76:24 CNGdiesel ratio was the focus of the experiment since here is where the most incomplete combustion gas emissions occur.

The Reuse of Exhaust Gases

Various diesel infusion times ranging from 30 degrees CA a.t.d. to top dead center (TDC) and EGR ratios up to 50% were tested. For this reason, the maximum EGR rate was set at 50% due to the correlation between higher EGR rates and volatile oxidation and poor thermal performance.

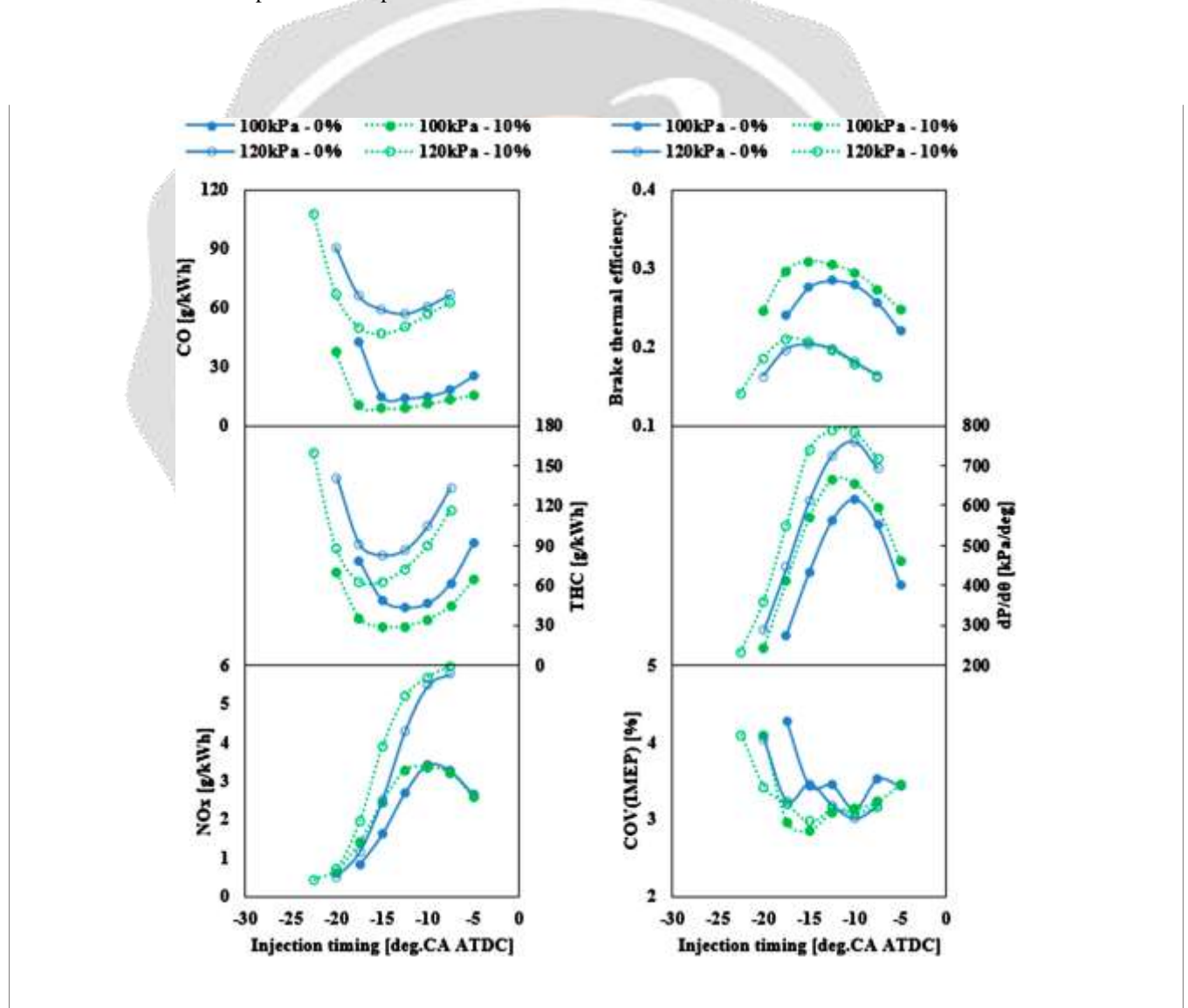


Figure 14: Typical emissions and combustion efficiency at varying diesel injection times, inlet pressure, and EGR levels

There is a comparison of EGR rates, diesel injection timings, emissions, and efficiency in Figure 13. Reduced CO and THC levels at 40% EGR lead to higher levels of oxidation and BTE. Bypassing the EGR chiller and going straight to the turbocharger, Hot-EGR boosts the intake charge temperature by 10 to 90 degrees Celsius, encouraging oxidation. Oxidation performance, CO, and THC generation are also affected by injection duration, with the lowest emissions seen between 17.5 and 12.5°C A ATCD.

It was shown that increasing EGR by 50% had little effect on reducing CO and THC emissions. Slightly more cases with early diesel infusion were found, suggesting that lower oxygen rates inside the cylinder may exacerbate oxidation. With an EGR rate of 50%, NO_x emissions are lowered and the impact of injection time is mitigated. High EGR rates lower dp/d and improve COV in engines.

Intake-boosting

There was a comparison between low-load intake enhancement with and without EGR in terms of its effect. With an intake pressure of 120 kPa, it was challenging to achieve high EGR rates, thus 10% was employed instead. The output data on emissions from boosted instances are comparable to those from non-boosted instances. Emissions are amplified in the early stages of diesel injection when a case has been turbocharged. The IMEP COV figure demonstrates that the COV does not increase for either the boosted or non-boosted cases, indicating that changes to the oxidation cycle cannot be responsible for the observed increase in emissions. CO and THC levels probably went up, but BTE went down, because of the very lean CNG-air mixture. Low-load boosting in a CNG-diesel dual flex-engine is inefficient. Increasing emissions while decreasing COV of IMEP rates is possible if the engine is slowed to reduce intake pressure.

CONCLUSIONS

The article presents research on dual-fuel oxidation from both experimental and simulated perspectives. Different engine designs, including those with one, two, or more cylinders, were analyzed in this study. Computational fluid dynamics (CFD) simulations were run using a highly linked structural model to learn more about oxidation. Low-load oxidation and emissions efficiency were the primary foci of the study, with attention paid to the impact of diesel infusion duration, volume, and pattern, as well as alternate airpath approaches including EGR and boosting.

Increased efficiency in diesel injection has decreased NO_x emissions and enhanced the engine's thermal efficiency. According to the CFD study, methane makes up the majority of low-load unburned hydrocarbon emissions. Using a split diesel injection strategy did not improve emissions reduction and instead increased unburned CH₄, which exacerbated THCs. With hot EGR, both NO_x and unburned species were decreased while low-load thermal efficiency was improved. The increased unburned pollutants and decreased thermal efficiency of the engine meant that inlet boosting did not help performance or emissions.

ACKNOWLEDGEMENT

All the praise go to Almighty God, The most beneficent and merciful for blessing the authors, The authors would like to give a special thanks to the Johnson and Sylvester Centre for African Research Engineer Library, for their Assistance in utilizing of the centre for Africa Research Engineering Library equipment to actualize our detailed results

REFERENCES

- Abani, N., and Reitz, R. D. (2007). Unsteady turbulent round jets and vortex motion. *Phys. Fluids*. 19 (12), 125102. doi:[10.1063/1.2821910](https://doi.org/10.1063/1.2821910)
- Abdelaal, M. M., and Hegab, A. H. (2012). Oxidation and emission characteristics of a natural gas-fueled diesel engine with EGR. *Energy Convers. Manag.* 64, 301–312. doi:[10.1016/j.enconman.2012.05.021](https://doi.org/10.1016/j.enconman.2012.05.021)
- Amsden, A. (1997). LA Report, LA-13313-MS. KIVA-3V: a block-structured KIVA program for engines with vertical or canted valves. doi:[10.1016/0375-6505\(82\)90028-1](https://doi.org/10.1016/0375-6505(82)90028-1)
- ANSYS, Inc. (2019). ANSYS 2019R1 Forte best practises. Canonsburg, PA:ANSYSInc.
- Cheenkachorn, K., Poompipatpong, C., and Ho, C. G. (2013). Performance and emissions of a heavy-duty diesel engine fuelled with diesel and LNG (liquid natural gas). *Energy* 53, 52–57. doi:[10.1016/j.energy.2013.02.027](https://doi.org/10.1016/j.energy.2013.02.027)
- Ciezki, H. K., and Adomeit, G. (1993). Shock-tube investigation of self-ignition of N-heptane-air mixtures under engine relevant conditions. *Combust. Flame*. 93 (4), 421–433. doi:[10.1016/0010-2180\(93\)90142-p](https://doi.org/10.1016/0010-2180(93)90142-p)

- Dimitriou, P., and Javaid, R. (2020). A review of ammonia as a compression ignition engine fuel. *Int. J. Hydrog. Energy*. 45, 7098–7118. doi:[10.1016/j.ijhydene.2019.12.209](https://doi.org/10.1016/j.ijhydene.2019.12.209).
- Dimitriou, P., and Tsujimura, T. (2017). A review of hydrogen as a compression ignition engine fuel. *Int. J. Hydrog. Energy*. 42 (38), 24470–24486. doi:[10.1016/j.ijhydene.2017.07.232](https://doi.org/10.1016/j.ijhydene.2017.07.232)
- IRENA (2019). *Hydrogen: a renewable energy Perspective*. Tokyo, Japan: IRENA.
- ISO 10054 (1998). *Internal oxidation compression ignition engines-apparatus for measurement of smoke from diesel engines operating under steady state conditions—Filter type smoke meter*. Berlin: Beuth Verlag.
- Karim, G. A. (2003). Oxidation in gas fueled compression: ignition engines of the dual fuel type. *J. Eng. Gas Turbines Power*. 125 (3), 827–836. doi:[10.1115/1.1581894](https://doi.org/10.1115/1.1581894)
- Kojima, H., Yoshida, A., Tsujimura, T., Fujino, T., Kawakita, S., Kondo, W., et al. (2016). A strategy of intake gas control for diesel dual fuel engine with natural gas and diesel fuel. *Trans. Soc. Automot. Eng. Jpn. Inc.* 47 (4), 889–894. doi:[10.11351/jsaeronbun.47.889](https://doi.org/10.11351/jsaeronbun.47.889)
- Kong, S.-C., and Reitz, R. D. (2002). Use of detailed chemical kinetics to study HCCI engine oxidation with consideration of turbulent mixing effects. *J. Eng. Gas Turbines Power*. 124 (3), 702–707. doi:[10.1115/1.1413766](https://doi.org/10.1115/1.1413766)
- Kusaka, J., Daisho, Y., Kihara, R., Saito, T., and Nakayama, S. (1998). “Oxidation and exhaust gas emissions characteristics of a diesel engine dual-fueled with natural gas,” in *Fourth international symposium COMODIA*. Kyoto, Japan, July 20–23, 1998
- Liang, L., Naik, C. V., Puduppakkam, K., Wang, C., Modak, A., Meeks, E., et al. (2010). Efficient simulation of diesel engine oxidation using realistic chemical kinetics in CFD. *SAE Technical papers*. doi:[10.4271/2010-01-0178](https://doi.org/10.4271/2010-01-0178)
- Liu, J., Yang, F., Wang, H., Ouyang, M., and Hao, S. (2013). Effects of pilot fuel quantity on the emissions characteristics of a CNG/diesel dual fuel engine with optimized pilot injection timing. *Appl. Energy*. 110, 201–206. doi:[10.1016/j.apenergy.2013.03.024](https://doi.org/10.1016/j.apenergy.2013.03.024)
- Lounici, M. S., Loubar, K., Tarabet, L., Balistrrou, M., Niculescu, D.-C., and Tazerout, M. (2014). Towards improvement of natural gas–diesel dual fuel mode: an experimental investigation on performance and exhaust emissions. *Energy* 64: 200–211. doi:[10.1016/j.energy.2013.10.091](https://doi.org/10.1016/j.energy.2013.10.091)
- Maricq, M. M., Chase, R. E., Xu, N., and Laing, P. M. (2002). The effects of the catalytic converter and fuel sulfur level on motor vehicle particulate matter emissions: light duty diesel vehicles. *Environ. Sci. Technol.* 36 (2), 283–289. doi:[10.1021/es0109621](https://doi.org/10.1021/es0109621)
- Mehl, M., and Curran, H. J. (2009). “Chemical kinetic modeling of component mixtures relevant to gasoline.” in *European oxidation meeting*, 1–6. Vienna, Austria, March 2, 2009
- Papagiannakis, R. G., Rakopoulos, C. D., Hountalas, D. T., and Rakopoulos, D. C. (2010). Emission characteristics of high speed, dual fuel, compression ignition engine operating in a wide range of natural gas/diesel fuel proportions. *Fuel* 89 (7), 1397–1406. doi:[10.1016/j.fuel.2009.11.001](https://doi.org/10.1016/j.fuel.2009.11.001)
- Patel, A., Song, C., and Reitz, R. D. (2004). Development and validation of a reduced reaction mechanism for HCCI engine simulations. *SAE Technical papers*. doi:[10.4271/2004-01-0558](https://doi.org/10.4271/2004-01-0558).
- Paul, A., Bose, P. K., Panua, R. S., and Banerjee, R. (2013). An experimental investigation of performance-emission trade off of a CI engine fueled by diesel-compressed natural gas (CNG) combination and diesel-ethanol blends with CNG enrichment. *Energy* 55, 787–802. doi:[10.1016/j.energy.2013.04.002](https://doi.org/10.1016/j.energy.2013.04.002)
- Reitz, R. D., and Beale, J. C. (1999). Modeling spray atomization with the Kelvin–Helmholtz/Rayleigh–Taylor Hybrid model. *Atom. Spr.* 9 (6), 623–650. doi:[10.1615/atomizspr.v9.i6.40](https://doi.org/10.1615/atomizspr.v9.i6.40)
- Sahoo, B. B., Sahoo, N., and Saha, U. K. (2009). Effect of engine parameters and type of gaseous fuel on the performance of dual-fuel gas diesel engines—a critical review. *Renew. Sustain. Energy Rev.* 13 (6–7), 1151–1184. doi:[10.1016/j.rser.2008.08.003](https://doi.org/10.1016/j.rser.2008.08.003)
- Selim, M. Y. E. (2001). Pressure-time characteristics in diesel engine fueled with natural gas. *Renew. Energy*. 22 (4), 473–489. doi:[10.1016/s0960-1481\(00\)00115-4](https://doi.org/10.1016/s0960-1481(00)00115-4)
- Shenghua, L., Longbao, Z., Ziyang, W., and Jiang, R. (2003). Oxidation characteristics of compressed natural gas/diesel dual-fuel turbocharged compressed ignition engine. *Proc. Inst. Mech. Eng. Part D J. Automob. Eng.* 217, 833–838. doi:[10.1177/095440700321700909](https://doi.org/10.1177/095440700321700909)
- Srinivasan, K. K., Krishnan, S. R., and Midkiff, K. C. (2006). Improving low load oxidation, stability, and emissions in pilot-Ignited natural gas engines. *Proc. Inst. Mech. Eng. Part D J. Automob. Eng.* 220 (2), 229–239. doi:[10.1243/09544070jauto104](https://doi.org/10.1243/09544070jauto104)
- Tsujimura, T., Aoyagi, K., Kurimoto, N., and Nishijima, Y. (2012). “Oxidation analysis for natural gas/diesel dual fuel engine,” in *Proceedings of the 8th international conference on modeling and diagnostics for advanced engine systems*, Fukuoka, Japan, July 23–26, 2012 COMODIA 2012, 380–385.

- Tsurushima, T. (2009). A new skeletal PRF kinetic model for HCCI oxidation. *Proc. Combust. Inst.* 32 (2), 2835–2841. doi:[10.1016/j.proci.2008.06.018](https://doi.org/10.1016/j.proci.2008.06.018)
- UNFCCC (2015). “Adoption of the Paris agreement,” in Conference of the parties on its twenty-first session. Paris, France, November 30–December 12, 2015
- Wang, Y., Ge, H.-W., and Reitz, R. D. (2010). Validation of mesh- and timestep-independent spray models for multi-dimensional engine CFD simulation. *SAE Int. J. Fuels Lubr.* 3, 277–302. doi:[10.4271/2010-01-0626](https://doi.org/10.4271/2010-01-0626)
- Wei, L., and Geng, P. (2016). A review on natural gas/diesel dual fuel oxidation, emissions and performance. *Fuel Process. Technol.* 142, 264–278. doi:[10.1016/j.fuproc.2015.09.018](https://doi.org/10.1016/j.fuproc.2015.09.018)
- Yang, B., Xi, C., Wei, X., Zeng, K., and Lai, M.-C. (2015). Parametric investigation of natural gas port injection and diesel pilot injection on the oxidation and emissions of a turbocharged common rail dual-fuel engine at low load. *Appl. Energy.* 143, 130–137. doi:[10.1016/j.apenergy.2015.01.037](https://doi.org/10.1016/j.apenergy.2015.01.037)

